Spin Singlet Formation in $MgTi_2O_4$: Evidence of a Helical Dimerization Pattern

M. Schmidt,[1,2] W. Ratcliff II,[3] P. G. Radaelli,[1,4] K. Refson,[1] N. M. Harrison,[5,6] and S. W. Cheong[3]
[1]ISIS Facility, Rutherford Appleton Laboratory, Chilton, Didcot, Oxon OX11 0QX, United Kingdom
[2]Department of Physics and Astronomy, Michigan State University, East Lansing, Michigan 48824, USA
[3]Department of Physics and Astronomy, Rutgers University, Piscataway, New Jersey 08854, USA
[4]Department of Physics and Astronomy, University College London, London WC1E 6BT, United Kingdom
[5]Department of Chemistry, Imperial College London, London SW7 2AY, United Kingdom
[6]CCLRC, Daresbury Laboratory, Warrington WA4 4AD, United Kingdom
(Received 4 August 2003; published 5 February 2004)

The transition-metal spinel $MgTi_2O_4$ undergoes a metal-insulator (M-I) transition on cooling below $T_{\text{M-I}} = 260$ K. A sharp reduction of the magnetic susceptibility below $T_{\text{M-I}}$ suggests the onset of a magnetic singlet state. Using high-resolution synchrotron and neutron powder diffraction, we have solved the low-temperature crystal structure of $MgTi_2O_4$, which is found to contain dimers with short Ti-Ti distances (the locations of the spin singlets) alternating with long bonds to form helices. Band structure calculations based on hybrid exchange density functional theory show that, at low temperatures, $MgTi_2O_4$ is an orbitally ordered band insulator.

DOI: 10.1103/PhysRevLett.92.056402 PACS numbers: 71.30.+h, 61.10.Nz, 61.12.Ld, 61.66.Fn

The interest in geometrically frustrated systems can be traced back to the work of Pauling [1] on the frozen disorder of crystalline ice. Frustration arises when geometrical constraints promote a locally degenerate ground state. In a periodic system with this local geometry, there exists a manifold of degenerate ground states, which may freeze on cooling forming ice or remain liquid down to the lowest temperatures due to quantum effects. A third possibility is that of a phase transition that lowers the local symmetry and lifts the degeneracy. In 1956, Anderson considered the ordering of charges or Ising spins on the B-site network of the spinel structure [2]. Spinels have the general formula AB_2X_4, where A and B are metals and X is an anion. The B site forms a network of corner-sharing tetrahedra, also known as the pyrochlore lattice, which is geometrically frustrated. It can be shown that Pauling's "ice rules" are equivalent to antiferromagnetic coupling between the spins or to nearest-neighbor Coulomb repulsion between equal charges. Anderson concluded that the spinels should have large low-temperature residual magnetic or configurational entropy, similar to ice. Also, he interpreted the Verwey transition of magnetite (Fe_3O_4, a half-filled mixed-valence spinel) [2] as an example of degeneracy-lifting transition. Almost perfect realizations of the "spin ice" concept were found much later in rare-earth pyrochlores such as $Ho_2Ti_2O_7$ [3]. One might in principle ask what would happen if the entities (spins, charges, etc.) at the nodes of the pyrochlore lattice had the tendency to form pairs. It is well-known, for example, that early transition metals in edge- or face-sharing octahedral coordination display strong cation-cation interaction, which often leads to dimerization and spin pairing [4]. The classic example of this behavior is VO_2 (rutile structure, V^{4+}, $3d^1$, $S = 1/2$), which undergoes a metal-insulator (M-I) transition at 340 K, associated with a structural transition from the high-temperature tetragonal structure to a monoclinic structure containing dimers with short V-V distances (2.65 Å) [5]. The magnetic susceptibility shows Curie-Weiss behavior above T_c and a nearly constant Van Vleck-like contribution below T_c, which is due to the formation of spin singlets associated with the V-V dimers. The rutile structure has a strong one-dimensional character, due to the presence of chains of edge-sharing octahedra running along the tetragonal c axis. Therefore, the transition in VO_2 can be described as a classic Peierls transition, associated with the splitting of the d band into bonding and antibonding branches [6].

In addition to early transition metals, low-spin cations with higher t_{2g} orbital occupancy can also form dimers. Recently, we have solved the low-temperature structure of the mixed-valent $CuIr_2S_4$ spinel [7], which displays simultaneous M-I, paramagnetic-diamagnetic, and structural transitions at 230 K. In $CuIr_2S_4$, iridium has an average oxidation state of 3.5 +, and half of the Ir ions were found to form short metal-metal bonds in the low-temperature insulating phase, giving rise to simultaneous charge ordering and dimerization. $MgTi_2O_4$ is another spinel with closely related phenomenology. In this compound, Ti is in the 3+ oxidation state with the $3d^1$ electronic configuration and $S = 1/2$, which makes it a strong candidate for the observation of dimerization in a single-valence system. In fact, $MgTi_2O_4$ undergoes a M-I transition on cooling below $T_{\text{M-I}} = 260$ K, accompanied by a strong decrease of the magnetic susceptibility and a transition to a tetragonal structure [8]. In this Letter, we report the solution and refinement of the low-temperature crystal structure of $MgTi_2O_4$, as obtained from synchrotron x-ray and neutron powder diffraction data, and the results of electronic structure calculations based on the structural data. The structure was found to contain dimers with short Ti-Ti distances (2.85 Å), the locations of the spin singlets. The dimer ordering leads to the formation of helical chains of short and long bonds running along the tetragonal *c* axis, a unique example of a chiral ordering of the spinel structure. The electronic structure is consistent with the opening of a 1 eV gap and the absence of magnetic moments and enables one to interpret the crystal structure in terms of orbital ordering.

$MgTi_2O_4$ powder samples were prepared by solid-state reaction of MgO, TiO_2, and elemental Ti powder mixture sealed under vacuum in a silica tube. The reactants were sintered at 1080 °C several times, followed by grinding in a glove box to increase homogeneity. Measurements of electrical resistivity and magnetic susceptibility of our sample produced results similar to those reported by Isobe and Ueda [8]. Synchrotron x-ray powder diffraction patterns of $MgTi_2O_4$ were collected on beam line ID31 at the European Synchrotron Radiation Facility in Grenoble, France, using a multianalyzer, parallel beam geometry at a wavelength of 0.5 Å. The sample was sealed in a 0.5 mm glass capillary and cooled down to 275 K (above the transition) and 200 K (below the transition) using a He blower. Medium- and high- resolution neutron powder diffraction patterns were collected at the Rutherford Appleton Laboratory in Chilton, UK using the GEM and HRPD instruments, respectively. High-resolution patterns were collected at 200 and 275 K, while medium-resolution data were collected in the 20–275 K temperature range in 20 K steps. For the neutron experiments, $MgTi_2O_4$ was sealed in a 6 mm vanadium can under Ar atmosphere and cooled by means of a closed cycle refrigerator. The neutron sample resulted from the second synthesis batch and was purer than the x-ray sample.

Comparison of the 275 and 200 K x-ray diffraction patterns confirmed the cubic-tetragonal phase transition and enabled us to identify most of the impurity peaks (mainly Ti_2O_3 and MgO) present in the pattern at the background level. A portion of the 200 K x-ray diffraction pattern is presented in Fig. 1(lower panel). Apart from the tetragonal splitting of the main Bragg peaks, a series of weak superlattice reflections also appear in the pattern. These can all be indexed on the $(a_c/\sqrt{2}) \times (a_c/\sqrt{2}) \times a_c$ primitive tetragonal unit cell, having half the volume of the cubic spinel cell. The extinction conditions uniquely identify a pair of enantiomorphic, noncentrosymmetric space groups, $P4_12_12$ and $P4_32_12$, which are equivalent except for their chirality. The atomic coordinates in the new space group can be freely refined based on the x-ray data, yielding a structural model that was further refined based on the neutron powder diffraction data. The final structural refinement was based on the combined GEM and HRPD data sets (a portion of the former is shown in the inset to Fig. 1), and the results at 200 K (tetragonal phase) and 275 K (cubic phase) are presented in Table I. Inclusion of the x-ray data slightly degrades the quality of the Rietveld fit, because of selective broadening of the superlattice reflections in the tetragonal phase; however, the calculated intensities of both main peaks and satellites are in excellent agreement with the x-ray results.

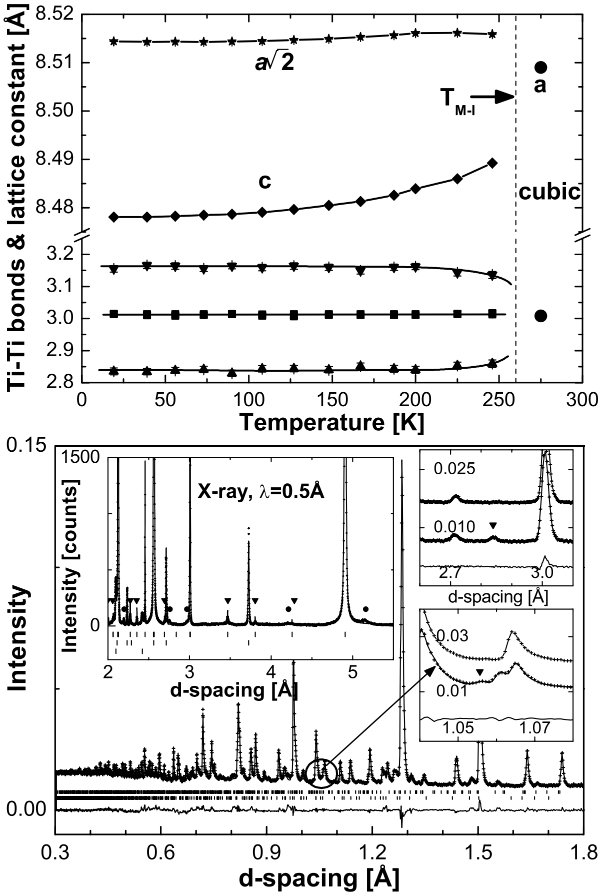

FIG. 1. Bottom: neutron and x-ray diffraction patterns of tetragonal $MgTi_2O_4$ at 200 K. The pattern was collected using the GEM 154° bank. The top to bottom rows of ticks mark the positions of $MgTi_2O_4$ and Ti_2O_3 Bragg peaks, respectively. Right-hand side insets: portions of GEM patterns from the 63° and 154° banks showing $MgTi_2O_4$ in the cubic state (top) and a refined tetragonal pattern. The down triangles mark reflections violating the body-centering condition. Left-hand side inset: the synchrotron x-ray diffraction pattern of $MgTi_2O_4$ at the background level (the strongest line has an amplitude of 32 000 counts). The top to bottom rows of ticks mark the positions of $MgTi_2O_4$, Ti_2O_3, and MgO Bragg peaks, respectively. The triangles mark the superlattice reflections; the circles mark an unidentified impurity. Top: The tetragonal lattice constants of $MgTi_2O_4$ and Ti-Ti bond lengths as functions of temperature derived from medium-resolution (GEM) data. The solid lines are guides for the eye. The data were corrected using lattice parameters derived from the x-ray experiment.

The tetragonal structure of $MgTi_2O_4$, as derived from the refinement of the 200 K data, is shown in Fig. 2. The

TABLE I. Lattice constants, fractional coordinates of atoms, and bonds in $MgTi_2O_4$ at 200 K ($P4_12_12$) and 275 K ($Fd\bar{3}m$). The parameters originate from the Rietveld refinement of high- and medium-resolution neutron powder diffraction patterns. The data were corrected using lattice constants derived from the x-ray experiment.

200 K		x	y	z	U_{iso} (Å^2)
Ti	8b	−0.0089(5)	0.2499(9)	−0.1332(4)	0.0125(2)
Mg	4a	0.7448(3)	0.7448(3)	0	0.0073(2)
O(1)	8b	0.4824(2)	0.2468(3)	0.1212(2)	0.0064(2)
O(2)	8b	0.2405(3)	0.0257(2)	0.8824(2)	0.0035(2)

$a = 6.022\,01(1)$ Å, $c = 8.484\,82(2)$ Å, $R_{wp} = 0.0467$, $R_p = 0.0637$

275 K		x	y	z	U_{iso} (Å^2)
Ti	16d	1/2	1/2	1/2	0.0117(1)
Mg	8a	1/8	1/8	1/8	0.0069(1)
O	32e	0.259 20(2)	0.259 20(2)	0.259 20(2)	0.005 22(5)

$a = 8.509\,027(5)$ Å, $R_{wp} = 0.0402$, $R_p = 0.0267$

Bond (Å)	Cubic, 275 K	Tetragonal, 200 K
Ti-Ti	3.008 43(1) × 6	2.853(7) × 1 3.007(5) × 2, 3.0147(3) × 2 3.157(7) × 1
Ti-O	2.0520(2) ×6	2.031(5), 2.026(5), 2.024(5) 2.083(5), 2.138(4), 2.020(4)

structure contains only one Ti site, ruling out the possibility of charge disproportionation. However, the center of symmetry at the Ti site is lost, so that Ti moves away from the center of the TiO_6 octahedron, and the six nearest-neighbor Ti-Ti distances become inequivalent. Two out of six Ti-Ti bonds [$s = 2.853(7)$ Å and $l = 3.157(7)$ Å] differ substantially from the Ti-Ti distance found in the cubic $MgTi_2O_4$ [3.008 43(1) Å]. The shortest distance is comparable to the close-contact distance in Ti metal (2.896 Å at room temperature), suggesting the formation of a metal-metal bond. It should be noted that the intradimer distance in VO_2 is 2.654 Å [5], which is also comparable to the V-V distance in V metal (2.61 Å). In the cubic spinel structure (inset of Fig. 2), the TiO_6 octahedra form edge-sharing "ribbons," so that the Ti-Ti bonds run in straight lines along six equivalent $[110]_c$ directions. In the tetragonal structure, both the short and the long bonds run along four directions ($[011]_c$, $[01\bar{1}]_c$, $[10\bar{1}]_c$, and $[101]_c$) of the cubic structure ($[112]_t$ direction), alternating with one of the intermediate bonds [$i_1 = 3.007(5)$ Å] in the sequence "s-i_1-l-i_1." Ti-Ti-bond lines running along the $[100]_t$ direction ($[110]_c$, $[1\bar{1}0]_c$) are entirely made up of the other type of intermediate bonds [$i_2 = 3.0147(3)$ Å]. Neither of the Ti-Ti-bond lines is perfectly straight, the Ti-Ti-Ti bond angle being 174.7(2)° and 178.3(1)° along the $[100]_t$ and $[112]_t$ directions, respectively. Refinements of the temperature-dependent neutron data indicate that the phase transition is abrupt, with no coexistence region between the two phase (Fig. 1, upper panel). This is reflected in the splitting of the Ti-Ti bond lengths, which is about 80% of the full value at 250 K and is fully saturated below 200 K.

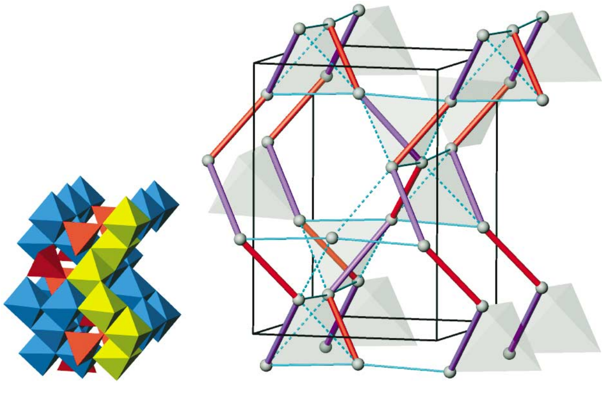

FIG. 2 (color). The Ti-Ti bond structure in tetragonal $MgTi_2O_4$ at 200 K. The red and purple bonds represent the shortest (dimerized) and the longest bonds in the $MgTi_2O_4$ structure, respectively. The dashed and solid blue bonds mark the intermediate $i_1 = 3.007(5)$ Å and $i_2 = 3.0147(3)$ Å Ti-Ti distances, respectively. A portion of the Ti tetrahedral connectivity is also shown. The inset shows a fragment of the spinel structure in the same orientation, visualized using cation-anion polyhedra. One of the "helices" is outlined in yellow.

From the topological point of view, the most interesting aspect of the $MgTi_2O_4$ low-temperature structure is the dimerization pattern of the alternating short and long bonds. Here, the chiral nature of the space group is clearly revealed in the formation of "s-l-s-l helices" running along the c axis (Fig. 2). With our choice of space group, the helices are left-handed, but the right-handed space group $P4_32_12$ is also an allowed solution. Several authors have pointed out the relevance of spin chirality for magnetism and transport on a pyrochlore lattice [9–11]. However, our observation of chirality in the structural sector of a pyrochlore lattice is extremely unusual and immediately raises two issues. First, it is interesting to consider whether the chiral dimerization pattern is in any way related to the geometrical frustration of the pyrochlore lattice. On this point, one should notice that, once the system "decides" to dimerize, the topology of the problem changes drastically: the relevant lattice is no longer the pyrochlore lattice itself, but its "medial" (or bond center) lattice at 1/6 filling (only one bond out of six is a dimer). Each Ti atom can be involved only in one dimer; therefore, one occupied dimer site precludes the occupancy of ten neighboring bonds. At such low filling, this rule clearly leads to a highly degenerate ground state, but, arguably, the system is no longer frustrated because the *local* degeneracy is absent. Second, the nature of the spin singlet state needs to be further investigated. To this effect, we have carried out band structure calculations using the CRYSTAL code [12]. All electron triple valence basis sets were used in which three independent radial functions are included for all valence states [13]. Electronic exchange and correlation are approximated using hybrid exchange density functional theory in which a component of the nonlocal Fock exchange is included with the local exchange and correlation approximated within the generalized gradient approximation (GGA) resulting in the B3LYP functional [14,15]. This functional is currently very widely used in molecular studies as it yields ground state energy significantly more reliably than GGA functionals. Here it is preferred to GGA as the component of the Fock exchange cancels in part the erroneous electronic self-interaction inherent in GGA functionals and thus the B3LYP approximation yields a reliable estimate of the band gap in a wide range of materials, including strongly interacting transition-metal oxides [16]. We note that initial calculations based on a GGA description failed to reproduce the opening of the band gap in the tetragonal phase. The computed projected densities of states (DOS) are plotted in Fig. 3 for the cubic and tetragonal structures; the latter was found to have a lower total energy than the former, as observed experimentally. In the cubic phase, the states just below the Fermi energy E_F form a highly dispersive, twofold degenerate band. This band is a common feature of many early transition-metal spinels [17] and originates mainly from $3d$-t_{2g} titanium orbitals, with the $3d_{xy}$, $3d_{xz}$, and $3d_{yz}$ participating equally in each energy level. In $MgTi_2O_4$, the Fermi energy lies in a deep "trough," where this band partially overlaps with more localized states at higher energy (also of t_{2g} origin), which accounts well for the poor metallic properties at room temperature. In the tetragonal, low-temperature phase the situation is radically different: four new bands with $3d_{xz}$ and $3d_{yz}$ contributions *only* are split off below the main t_{2g} band. Complete filling of these bands with eight electrons in the double cell results in a gap of about 1 eV, in good agreement with the electrical conductivity [8], while the $3d_{xy}$ states are pushed to higher energy. These results are readily interpreted on the basis of the observed crystal structure by noting that the short Ti-Ti bonds have the same orientation as the occupied t_{2g} orbitals, alternating between the $3d_{yz}$ ($[011]_c, [01\bar{1}]_c$), and $3d_{xz}$ ($[10\bar{1}]_c, [101]_c$) directions on different sites. This is consistent with orbital ordering, and with the short bonds becoming the location of zero-spin Hund-Mulliken (molecular-orbital-like) singlets. The driving force for behind stabilization of the $MgTi_2O_4$ tetragonal structure is the tendency to form dimers and the Jahn-Teller distortion is playing a minor role.

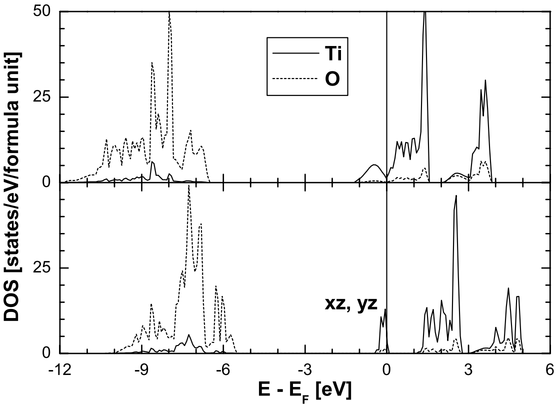

FIG. 3. Electronic DOS for the cubic (top) and the tetragonal (bottom) $MgTi_2O_4$. The contributions of Ti and O are indicated with different line styles (the Mg contribution to DOS is negligible in this energy range). The vertical line marks the Fermi energy.

In summary, we have determined the crystal and electronic structures of the high- and low-temperature phases of $MgTi_2O_4$. At low temperatures, the Ti atoms dimerize forming an unusual chiral pattern. This results in orbital ordering, and in the opening of a gap between the fully occupied and unoccupied levels, in good agreement with the transport and magnetic properties of $MgTi_2O_4$.

We thank Daniel Khomskii for fruitful discussions of this work and François Fauth for his help with the ESRF synchrotron experiment. This work was supported in part by U.S. DOE Office of Science Grant No. DE-FG02-97ER45651 and by NSF Grant No. DMR-0103858.

[1] L. Pauling, J. Am. Chem. Soc. **57**, 2680 (1935).
[2] P.W. Anderson, Phys. Rev. **102**, 1008 (1956).
[3] S.T. Bramwell and M. J. P. Gingras, Science **294**, 1495 (2001).
[4] J. B. Goodenough, Phys. Rev. **117**, 1442 (1960).
[5] G. Andersson, Acta Chem. Scand. **10**, 623 (1956).
[6] R. M. Wentzcovitch, W.W. Schultz, and P. B. Allen, Phys. Rev. Lett. **72**, 3389 (1994).
[7] P.G. Radaelli, Y. Horibe, M.J. Gutmann, H. Ishibashi, C.H. Chen, R.M. Ibberson, Y. Koyama, Y.S. Hor, V. Kiryukhin, and S.W. Cheong, Nature (London) **416**, 155 (2002).
[8] M. Isobe and Y. Ueda, J. Phys. Soc. Jpn. **71**, 1848 (2002).
[9] K. Ohgushi, S. Murakami, and N. Nagaosa, Phys. Rev. B **62**, R6065 (2000).
[10] S. Yoshii, S. Iikubo, T. Kageyama, K. Oda, Y. Kondo, K. Murata, and M. Sato, J. Phys. Soc. Jpn. **69**, 3777 (2000).
[11] Y. Taguchi, Y. Oohara, H. Yoshizawa, N. Nagaosa, and Y. Tokura, Science **291**, 2573 (2001).
[12] V.R. Saunders, R. Dovesi, C. Roetti, M. Causà, N.M. Harrison, R. Orlando, and C.M. Zicovich-Wilson, *CRYSTAL98 Users's Manual* (University of Torino, Torino, 1999).
[13] Http://www.ch.unito.it/ifm/teorica/Basis_Sets/mendel.html.
[14] A. D. Becke, J. Chem. Phys. **98**, 5648 (1993).
[15] C. Lee, W. Yang, and R.G. Parr, Phys. Rev. B **37**, 785 (1988).
[16] J. Muscat, A. Wander, and N. M. Harrison, Chem. Phys. Lett. **342**, 397 (2001).
[17] S. Satpathy and R.M. Martin, Phys. Rev. B **36**, 7269 (1987).